Air-Cooled Heat Exchanger Performance for R410A

T. Ebisu
Daikin Industries

K. Yoshida
Daikin Industries

K. Torikoshi
Daikin Industries

AIR-COOLED HEAT EXCHANGER PERFORMANCE FOR R410A

Takeshi Ebisu, Kaori Yoshida and Kunikazu Torikoshi

Mechanical Engineering Laboratory, Daikin Industries, Ltd.
1304 Kanaoka-cho, Sakai, Osaka 591 Japan

ABSTRACT

The present study was carried out experimentally to evaluate the air-cooled heat exchanger performances for R410A. The experiments were performed with the heat exchangers for three different refrigerant flow circuits. Measurements were made on heat exchanger performances for R410A and R22 in cooling and heating modes. The results obtained in the present study showed that the difference of the heat exchanger performance for R410A in cooling mode significantly occurred in individual flow circuits. Comparison results between for R410A and R22 showed that the heat exchanger performance for R410A was higher than that for R22. In heating mode, the heat exchanger performance for R410A was insensitive to the change in circuits, and the heat exchanger performance for R410A was almost the same as that for R22. The difference of individual heat exchanger performance for three different flow circuits was explainable by the reason that the lower pressure difference of refrigerant, the larger is heat flux at the surface of the heat exchanger.

NOMENCLATURE

A :	Surface area of the heat exchanger	**subscript**	
Cp :	Specific heat of air	a :	air
G :	Refrigerant flow rate	c :	condensation
ΔP :	Pressure difference	e :	evaporation
Q :	Heat capacity	i :	inlet
T :	Temperature	o :	outlet
ΔT :	Temperature difference	r :	refrigerant
h :	Enthalpy	s :	saturation
Δh :	Enthalpy difference	SC :	subcooling
u :	Air velocity	SH :	superheat
x :	Quality	w :	wall

INTRODUCTION

The 4th amendment of the Montreal Protocol made at Copenhagen Conference in 1992 has called for a new phaseout schedule of HCFCs, including R22, due to the enforced protection of the stratospheric ozone layer. A production cap for HCFCs has just started from January 1, 1996. Concerning the candidates for R22 used in air-conditioning machines, a ternary zeotropic mixture R407C and a binary azeotropic mixture R410A are currently nominated to be the promising replacements from the view point of environmental friendship such as zero ODP and nonflammability.

Besides the basic characteristics such as thermal properties, lubrication and flammability, information on the heat transfer characteristics inside heat transfer tubes and the salient features of air-cooled heat exchanger performances for the alternative refrigerants have been the subjects of fundamental importance to design air-cooled heat exchangers installed into air-conditioning machines. The authors have provided with much information on the evaporation and condensation heat transfer characteristics inside a horizontal tube for the alternative refrigerants such as R134a(1), R32(2), R32/134a(3), R407C(4) and R410A(5).

For R407C, which is one of the most promising replacements for R22, the report(4) by the authors indicated that the evaporation and condensation heat transfer coefficients inside a horizontal heat transfer tube fell about 30 - 50% below those for R22. In addition to the heat transfer characteristics inside a heat transfer tube, evaluation of heat exchanger performance is needed for designing the optimum air-conditioners and heat pumps with R407C. The authors have conducted the experimental study(6) concerning the air-cooled heat exchanger performance for R407C. The experimental results confirmed that the heat exchanger performances for R407C were consistent with those for R22 in the cooling mode, while the heat exchanger performances for R407C in the heating mode were higher than those for R22.

Regarding another promising alternative refrigerant R410A, the authors(5) presented the heat transfer data during evaporation and condensation in a heat transfer tube. The heat transfer coefficients for R410A were found to be almost the same as those for R22, and the comparisons of the pressure drop between R410A and R22 showed the significant result that the pressure drop for R410A was about 25 - 35% lower than that for R22. Although the lower pressure drop inside a heat transfer tube for R410A gives considerable advantage to the heat exchanger performance, it is difficult to evaluate quantitatively the effects of the pressure drop on the heat exchanger performance for R410A. This is because the pressure drop of the refrigerant inside the tube results in the change in the evaporation/condensation pressures, the surface temperature of the heat exchanger and the refrigerant flow rate.

The objective of the present study is to evaluate experimentally the air-cooled heat exchanger performances for R410A. In the present study, the experiments were performed with the heat exchangers for three different refrigerant flow circuits. The heat exchangers to be tested are actually used in the inner unit of the residential air-conditioning machine with 2.5kW. Measurements were made on heat exchanger performances for R410A in cooling and heating modes. The heat exchanger performance for R22 was also examined in order to compare the heat exchanger performances between for R410A and R22.

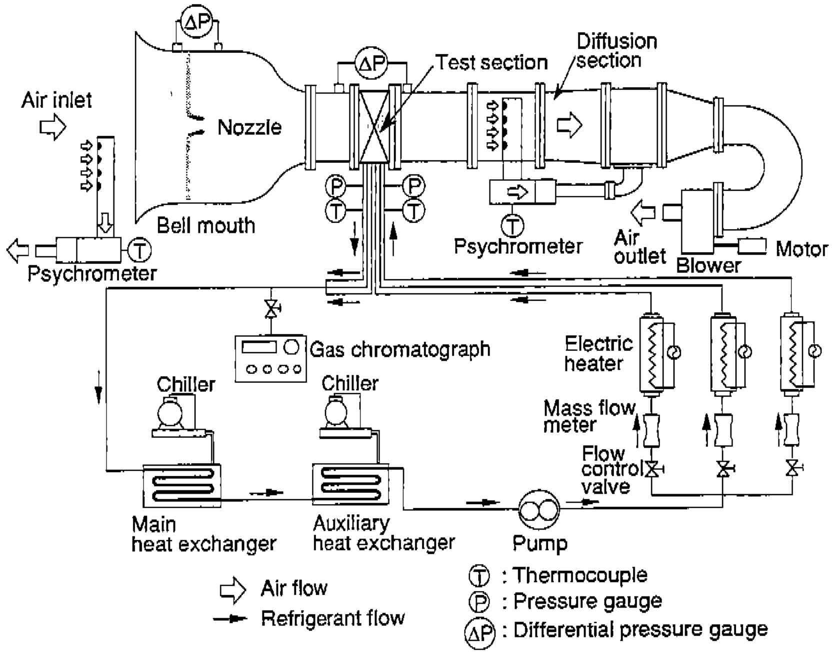

Figure 1 Schematic diagram of experimental apparatus

EXPERIMENTS

Experimental Apparatus

A schematic diagram of the experimental apparatus is shown in Figure 1. The apparatus is designed to draw the room air over the test section, while supplying the refrigerant into the heat exchanger.

The wind tunnel illustrated upper side in Figure 1 was set up in the hermetic testing room in which both of temperature and humidity of air are maintained to be the desired conditions. The wind tunnel was composed of the bell mouth section, test section, diffusion section and blower. The bell mouth was designed to provide air velocity distributions within 5% in the test section. The room air was admitted to the wind tunnel by a blower, and the air flow rate was determined from the measurement with the calibrated nozzle. In order to measure the temperature and humidity at the inlet and outlet of the test section, two psychrometers were located near to the wind tunnel. Each sampling device of the psychrometer was mounted upstream of the wind tunnel entrance and downstream of the test section, respectively. The dry-bulb and wet-bulb temperatures in the psychrometers were taken by the Pt resistance sensors within an accuracy of 0.02K. In order to reduce heat losses from the air side of the test section, all walls of the test section and the wind tunnel were insulated with 5cm styrofoam.

The refrigerant loop is shown in lower side in Figure 1. The loop consisted of a pump, mass flow meters, electric heaters and two heat exchangers. In place of a compressor, the pump was used to circulate the refrigerant into the loop without lubricant. The main heat exchanger was installed in the refrigerant loop to regulate the desired pressure of the refrigerant, while the auxiliary heat exchanger was used to liquidize the refrigerant flowing into the pump. The mass flow meters and flow regulating valves were connected downstream of the pump to allow the desired

Table 1 Description of test heat exchanger

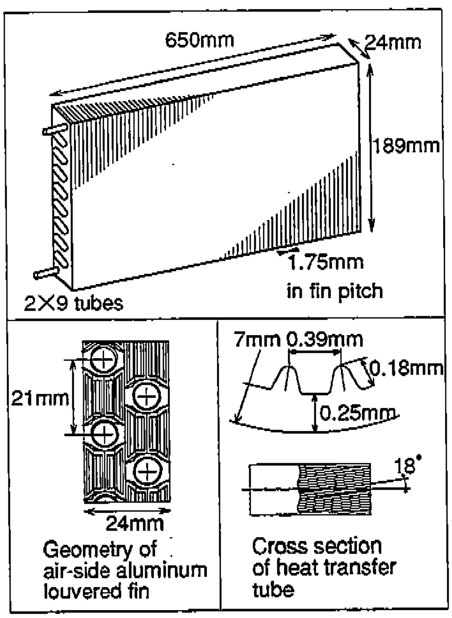

refrigerant flow rate. To control the quality and superheat of the refrigerant flowing into the test section, the electric heaters were located upstream of the test section. Gas chromatography was prepared to check the composition of the refrigerant mixture.

Description of Test Heat Exchanger

An appearance of the heat exchanger to be tested in the present experiments is shown in Table 1 with the geometrical information. Table 1 includes information on the fin and tube consisting of the test heat exchanger. The heat exchanger corresponds to the actual inner unit of the residential air-conditioning machine with 2.5kW. The heat exchanger, having 650×189mm in face area, was mounted into the test section of the wind tunnel and connected with the refrigerant loop to supply the refrigerant.

The heat transfer tubes of the test heat exchanger were positioned in a staggered array with two rows, schematically shown in Figure 2. In the present experiments, the heat exchangers for three different refrigerant flow circuits were employed to examine the effect of the tube length on the heat exchanger performance. The flow configurations of the refrigerant and air were also shown in Figure 2, respectively.

In order to measure both the pressures of the refrigerant at the inlet and outlet of the heat exchanger, the pressure taps in 0.5mm diameter were equipped at the inlet and outlet of the heat exchanger. Measurements of the refrigerant temperatures were made with the thermocouples. The thermocouples were located near the pressure taps. In addition, a total of 19 thermocouples was attached on the U-turn bends of the heat transfer tube to measure the tube wall temperatures along the length of the heat exchanger. The thermocouple reading data was utilized to obtain the surface temperature of the heat exchanger.

Experimental Conditions

Experimental conditions in cooling and heating modes are listed in Table 2. The experiments were conducted for air in velocity ranging from 0.7 to 1.3m/s in the face area of the heat exchanger.

The evaporation and condensation temperatures of the refrigerant were determined from the saturation temperature corresponding to the refrigerant pressures measured at the outlet and inlet of the test heat exchanger for evaporation and condensation, respectively. In the cooling mode, the refrigerant superheat, T_{SH}, was given as the temperature difference between the saturation temperature, T_e, and the measured refrigerant temperature, T_{ro}, while the refrigerant subcooling, T_{SC}, in the heating mode represented the temperature difference between T_s and T_{ro}. In the present experiments, T_e and T_c were maintained constant at 278K(5℃) and 313K(40 ℃), respectively. Further, both of T_{SH} and T_{SC} were held constant at 5K.

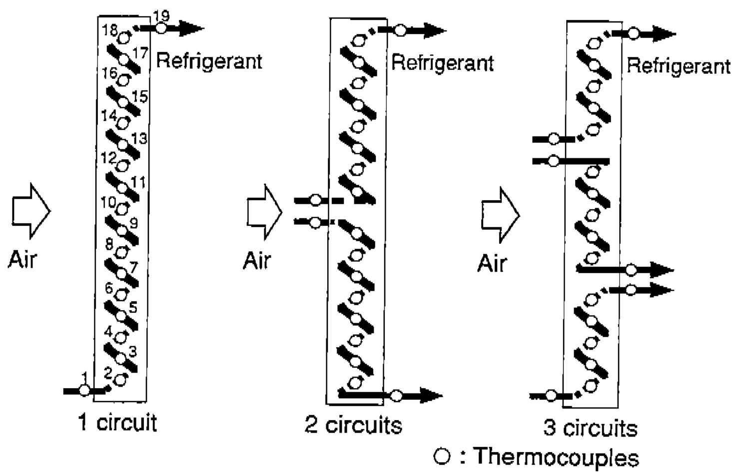

Figure 2 Tube arrangements of test heat exchangers

Data Reduction

The capacity of the heat exchanger, Q, was calculated with the following equation:

$$Q=G\times\Delta h \quad (1)$$

where G and Δh denote the refrigerant flow rate and the enthalpy difference between the inlet and outlet the refrigerant. Δh was defined by equations (2) and (3)

$$\Delta h=h_o-h_i \quad \text{for evaporation} \quad (2)$$

$$\Delta h=h_i-h_o \quad \text{for condensation} \quad (3)$$

On the other hand, Q was also obtained by the air side measurements :

$$Q=\rho\times C_p\times u\times A\times\Delta T \quad (4)$$

In the equation (4), ΔT represents the temperature difference between the air temperature at the inlet and outlet of the test section. Comparisons between the heat quantities in the air and refrigerant sides show that both values were in excellent agreement within 2%. Accordingly, the capacity of the heat exchanger was calculated from the

Table 2 Experimental conditions

		Cooling mode	Heating mode
Air side	Dry bulb temp.	300 (K)	283 (K)
	Wet bulb temp.	292 (K)	279 (K)
	Air face velocity	0.7, 1.0, 1.3 (m/s)	
Ref side	Saturation temp.	278 (K)	313 (K)
	Inlet	X=0.2	T_{SH}= 27 (K)
	Outlet	T_{SH}=5 (K)	T_{SC}= 5 (K)

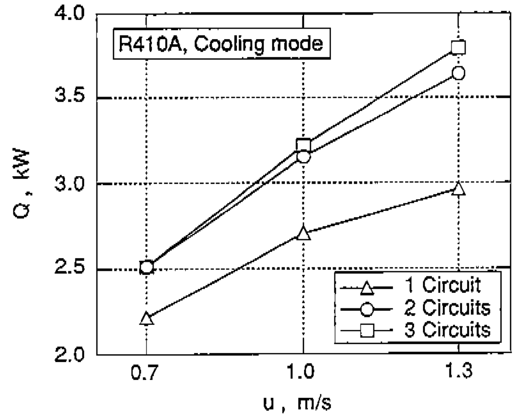

Figure 3 Effect of refrigerant flow circuit on the heat exchanger capacity for R410A

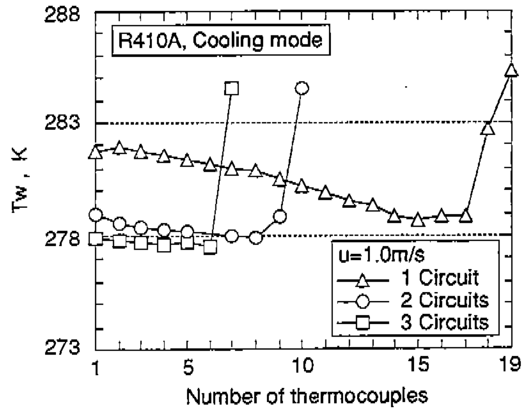

Figure 5 Effect of refrigerant flow circuit on tube wall temperature

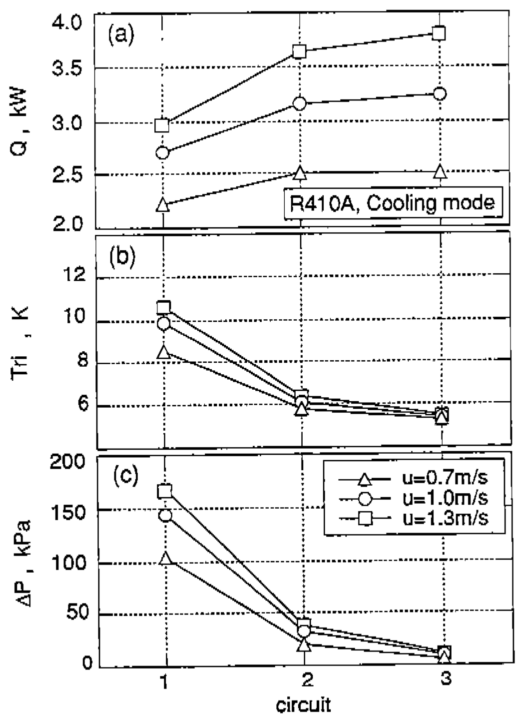

Figure 4 Experimental data as a function of refrigerant flow circuit

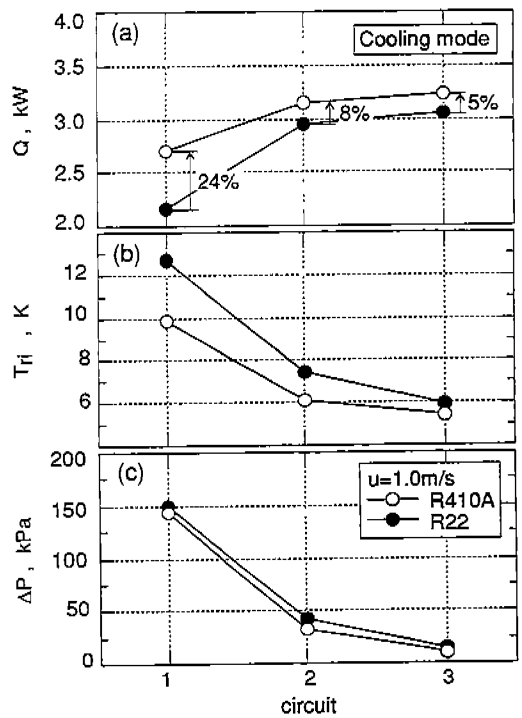

Figure 6 Comparison of data between for R410A and R22

refrigerant side in the present experiments.

RESULTS AND DISCUSSION

Cooling Mode

The performance results of the heat exchanger used as evaporator are shown in Figure 3, as a function of air velocity passing through the heat exchanger. In the figure, the data are given for R410A. The figure shows that the heat exchanger performances are dependent on the number of circuits, and the maximum performance is attainable for the 3 circuits in this study. Also comparisons among the results for three different refrigerant flow circuits at u=1.0m/s show that the heat exchanger performances for 2 and 3 circuits surpass that for 1 circuit by 17% and 19%, respectively.

In order to clarify the experimental findings, the data on heat capacity, Q, refrigerant temperature at the inlet of the heat exchanger, T_{ri}, and pressure difference between at the inlet and outlet of the heat exchanger, ΔP, are prepared in

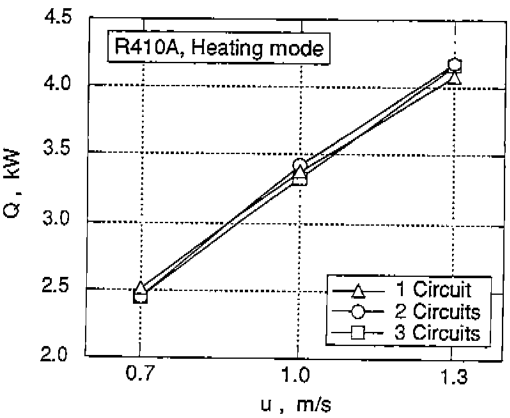

Figure 7 Effect of refrigerant flow circuit on the heat exchanger capacity for R410A

Figure 4. Figures 4(a), 4(b) and 4(c) corresponds to the results of Q, T_{ri} and ΔP, respectively. Figure 4(c) shows that ΔP decreases as the heat exchanger circuit increases. Decreasing ΔP results in the decrease of T_{ri} as shown in Figure 4(b). The decrease of T_{ri} brings about the decrease of the surface temperature of the heat exchanger. Eventually, the increased heat flux at the surface of the heat exchanger occurs when T_{ri} is decreased. The results in Figure 4(a) are explainable by the reason that the lower T_{ri}, the larger is heat flux.

Surface temperature distributions of the heat exchanger along the tube length for three different circuits are displayed in Figure 5. The figure is prepared for the purpose of confirming the reason above mentioned. The data in the figure are given for u=1.0m/s. As seen in the figure, the surface temperatures on the heat transfer tubes for 1 circuit are higher than those for 2 and 3 circuits.

Representative comparison results between for R410A and R22 are shown in Figures 6(a), 6(b) and 6(c) for u=1.0m/s. Figure 6(a) demonstrates that the heat exchanger performance for R410A is significantly higher than those for R22. The ratios of the heat exchanger performance for R410A to that for R22 depend on the number of circuit. For 1, 2 and 3 circuits, the ratios are about 24%, 8% and 5%, respectively. The results as shown in Figures 6(b) and 6(c) show that ΔP for R410A is smaller than that for R22, and that T_{ri} for R410A is lower than that for R22. Therefore, the results in Figure 6(a) are considered to be due to the reason that the lower T_{ri}, the larger is heat flux at the surface of the heat exchanger for R410A.

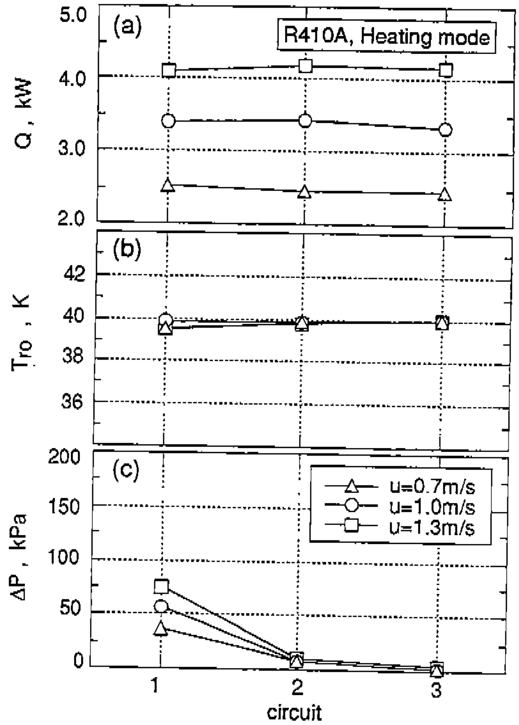

Figure 8 Experimental data as a function of refrigerant flow circuit

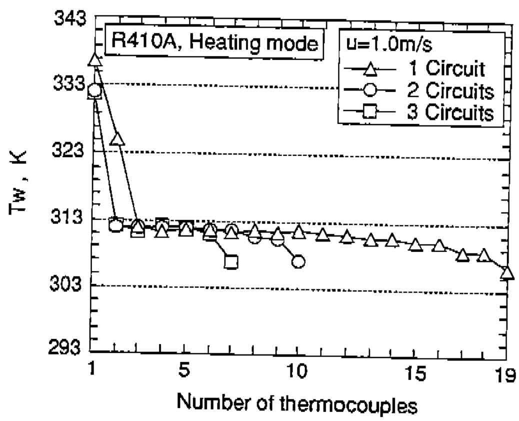

Figure 9 Effect of refrigerant flow circuit on tube wall temperature

Heating Mode

Figure 7 shows the performance results of the heat exchanger used as condenser for R410A. The heat exchanger performance results for three different refrigerant flow circuits exhibit to be unaffected by tube length of the heat exchanger.

To confirm the results different from those in cooling mode, the data for Q, T_{ro} and ΔP are prepared in Figures 8(a), (b) and (c), respectively. Figure 8(c) shows that ΔP decreases with increase in number of circuit. However, the value of ΔP is significantly smaller in heating mode when compared to that in cooling mode. Examination of Figure 8(b) reveals that the refrigerant temperatures at the outlet of the heat exchanger for three different circuits are independent on ΔP. From the figure, it is clear that the surface temperature of the heat exchanger maintains constant for all refrigerant flow circuits in the present experiments.

The surface temperature distributions along the tube length are shown in Figure 9. The figure reveals that the surface temperatures of the heat exchangers are almost the same among three different refrigerant flow circuits.

Figures 10(a), 10(b) and 10(c) show the comparisons of the experimental data between for R410A and R22. Figure 10(a) shows that the heat exchanger performance for R410A is almost same as that for R22. This is because ΔP and T_{ro} for R410A are similar to those for R22 as shown in Figure 10(b) and 10(c), respectively.

CONCLUSIONS

This study was carried out experimentally to evaluate the heat exchanger performance for R410A. Experiments were performed with the heat exchangers for three different refrigerant flow circuits. The findings obtained in the present experiments are as follows:

1. In cooling mode, the heat exchanger performances were significantly different from the individual circuits of the heat exchangers. The heat exchanger performances for 2 and 3 circuits surpassed that for 1 circuit by 17% and 19%, respectively. In particular, for the 1 circuit heat exchanger, comparison results between for R410A and R22 demonstrated that the heat exchanger performance for R410A was far above that for R22.
2. In heating mode, the heat exchanger performance results for three different refrigerant flow circuits exhibited to be insensitive to the change in the circuit corresponded to the change in the tube length of the heat exchanger. The heat exchanger performance for R410A was almost the same as that for R22.

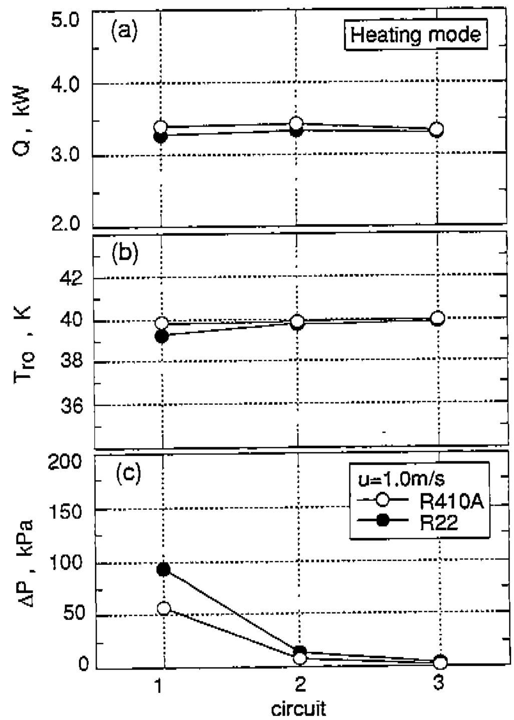

Figure 10 Comparison of data between for R410A and R22

REFERENCES

(1) Torikoshi, K., K. Kawabata and T. Ebisu, Heat transfer and pressure drop characteristics of HFC-134a in a horizontal heat transfer tube, Proceedings of 1992 International Refrigerant Conference at Purdue, (1992), Vol. 1, pp 167-176.

(2) Torikoshi, K. and T. Ebisu, In-tube condensation of alternate refrigerants, Proceedings of Condensation and Condenser Design, (1993), pp 593-600.

(3) Torikoshi, K. and T. Ebisu, Heat transfer and pressure drop characteristics of R134a, R32 and a mixture of R32/R134a inside a horizontal tube, ASHRAE Transactions (1993), Vol. 99, Part 2, pp 90-96.

(4) Ebisu, T. and K. Torikoshi, In-tube heat transfer characteristics of refrigerant mixtures of HFC-32/134a and HFC-32/125/134a, Proceedings of 1994 International Refrigeration Conference at Purdue, (1994), pp 293-298.

(5) Ebisu, T., K.Torikoshi and K. Okuyama, ASHRAE Transactions, to be submitted.

(6) Ebisu,T. and K. Torikoshi, Experimental studies on crossflow heat exchanger performance using non-azeotropic refrigerant mixture, Proceedings of 19th International Congress of Refrigeration 1995, (1995), Vol. 4a, pp 163-170.